Spatiotemporal Behavior of Drift Waves in LMD-U

Takuma YAMADA[1)], Sanae -I. ITOH[1)], Kenichiro TERASAKA[2)], Naohiro KASUYA[3)], Yoshihiko NAGASHIMA[1)], Shunjiro SHINOHARA[2)], Takashi MARUTA[2)], Masatoshi YAGI[1)], Shigeru INAGAKI[1)], Yoshinobu KAWAI[1)], Akihide FUJISAWA[3)] and Kimitaka ITOH[3)]

[1)] *Research Institute for Applied Mechanics, Kyushu University, Kasuga 816-8580, Japan*
[2)] *Interdisciplinary Graduate School of Engineering Sciences, Kyushu University, Kasuga 816-8580, Japan*
[3)] *National Institute for Fusion Science, Toki 509-5292, Japan*

In the LMD-U linear magnetized plasma, fluctuation measurements with multi-channel poloidal Langmuir probe arrays have been performed. The mean poloidal mode number of the fluctuation and its spread suggest the existence of broadband fluctuation, which is considered to be produced by nonlinear couplings. The broadband fluctuation develops into high poloidal mode number and high frequency region, which do not satisfy the linear dispersion relation of drift wave modes. The broadband fluctuation revealed small correlation time and poloidal length than the fluctuation peaks. Poloidal mode decomposed axial coherence was measured with two poloidal probe arrays. The axial coherence was strong both for the broadband fluctuation and fluctuation peaks.

Keywords: linear plasma, multi-probe, drift wave, turbulence, nonlinear coupling

1 Introduction

Recently, there has been an advance in the study of nonlinear interaction between drift wave turbulence and meso-scale structures such as zonal flows and streamers [1, 2]), and experiments in linear plasma devices have been in progress [3–10]. In these studies, complex wave patterns in poloidal direction have been observed (see also reports from toroidal plasma experiments, e.g., [11–14]). These advancements highlight the need to measure fluctuations at multiple spatial positions simultaneously. Fluctuation measurements using poloidal multi-probe arrays have been performed in linear plasmas and torus plasmas [3, 4, 6, 15].

In the LMD-U linear magnetized plasma [16], multi-point measurements of the ion saturation current and floating potential fluctuations using poloidal Langmuir probe arrays have been in progress. Drift wave modes driven by steep radial density gradient were identified, and a drift wave turbulence regime was achieved [17]. The poloidal mode numbers and frequencies of the drift wave modes were compared with the calculated linear dispersion relation of drift wave [18], and they were in a good agreement. Moreover, in a drift wave turbulence regime, quasi-modes and broadband components that do not satisfy the dispersion relation were found and suggested that they were produced by nonlinear couplings of parent modes [19]. In this article, we report the details about the broadband components found in the drift wave turbulence regime.

2 Poloidal Probe Arrays

We have performed a quasi-two-dimensional measurement of the ion saturation current fluctuation of the LMD-U lin-

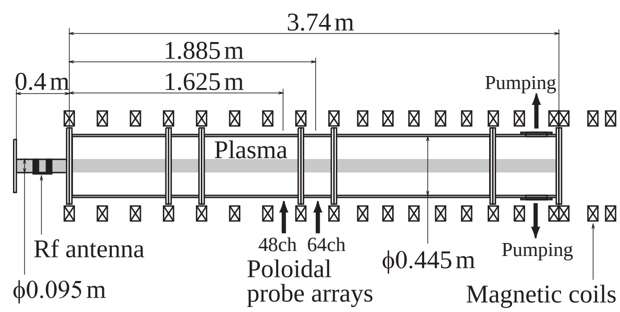

Fig. 1 Schematic view of the LMD-U linear plasma device, and the positions of the polodial probe arrays (64-channel and 48-channel).

ear plasma [16]. The schematic view of the LMD-U device is shown in Fig. 1. A linear magnetized plasma is created by an rf (the frequency of 7 MHz and the power of 3 kW) antenna in a quartz tube (the axial length of 0.4 m and the inner diameter of 0.095 m) with argon gas filled in. The plasma is guided along straight magnetic field created by magnetic coils surrounding the vacuum vessel to form a column shape. The axial length and inner diameter of the vacuum vessel are 3.74 m and 0.445 m, respectively.

There are two poloidal Langmuir probe arrays installed on LMD-U. A 64-channel poloidal probe array is installed at the axial position of 1.885 m and a 48-channel poloidal probe array is installed at 1.625 m. The tungsten probe tips of the 64-channel probe array are fixed at the measuring radius of 40 mm (the probe tips are 3.9 mm apart), and the position of the whole probe array is adjustable two-dimensionally in the plasma cross section. Therefore, the precise poloidal mode number of the fluctuation is available by this probe array [20]. The 48-channel probe array consists of 16 probe units, which are mov-

author's e-mail: takuma@riam.kyushu-u.ac.jp

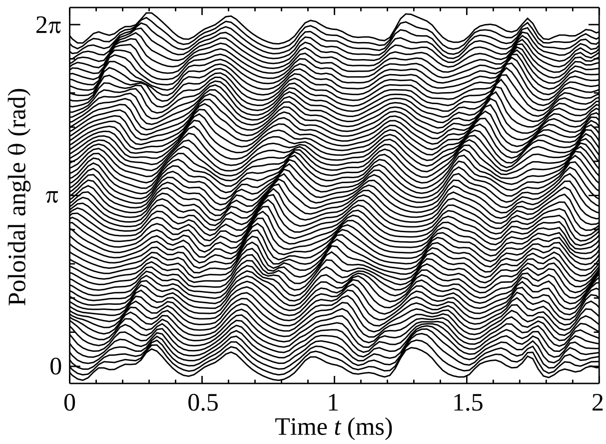

Fig. 2 Spatiotemporal behavior of the ion saturation current $I(\theta, t)$ measured with the 64-channel poloidal probe array.

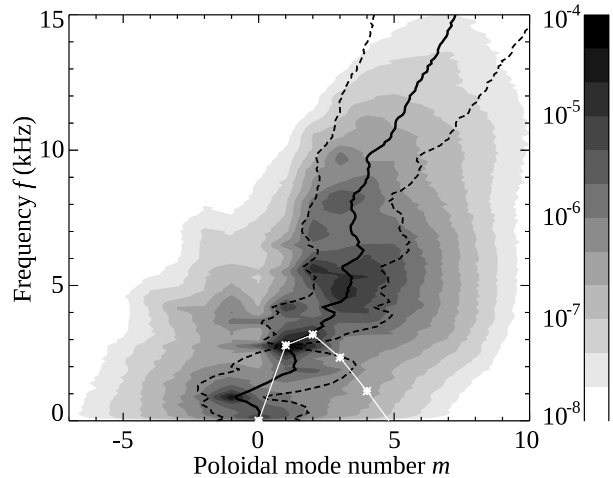

Fig. 3 Contour plot of the power spectrum $S(m, f)$ (arb. unit) over plotted with the calculated linear dispersion relation of drift waves (white asterisks). The solid black line shows the mean poloidal mode number, and the broken black lines show its spread.

able in the radial direction. Each probe unit has 3 tungsten probe tips. The probe tips line up to equal distance when the measuring radius is set to 40 mm (the probe tips are 5.2 mm apart). This probe array can measure the poloidal wave number and radial profile of the plasma fluctuation [17]. By these two poloidal probe arrays, the details of the broadband fluctuation and fluctuation peaks such as poloidal mode numbers, poloidal correlation lengths and poloidal mode decomposed axial correlations are measurable.

3 Spectral Analysis

The spatiotemporal behavior of the ion saturation current fluctuation varies by changing parameters from periodical coherent wave structure to turbulence regime, which consists of many fluctuation components with different poloidal mode numbers and frequencies [4]. In LMD-U, increasing the magnetic field (over 0.04 T) and decreasing the filled argon pressure (under 0.4 Pa) make the plasma into turbulence regime by affecting the density gradient and collision with neutrals [16]. Figure 2 shows the spatiotemporal behavior of the ion saturation current $I(\theta, t)$, where θ is the poloidal angle and t is the time, in the turbulence regime measured with the 64-channel probe array. The magnetic field was 0.09 T and the argon pressure was 0.27 Pa. The increasing direction of the poloidal angle θ corresponds to the electron diamagnetic direction. The spatiotemporal waveform consists of a number of fluctuation components. The main fluctuation is the flow in the electron diamagnetic direction with the frequency of about 3 kHz.

The spatiotemporal waveform in the turbulence regime can be decomposed into the poloidal mode number and frequency spaces by spectral analysis. By two-dimensional Fourier transformation (poloidal angle θ to poloidal mode number m, and time t to frequency f), $I(\theta, t)$ is transformed to $\hat{I}(m, f)$. Figure 3 shows the power spectrum $S(m, f) = \langle|\hat{I}(m, f)|^2\rangle/df$, where df is the frequency resolution and is 0.1 kHz in this case. The power spectrum $S(m, f)$ was an ensemble of 300 time windows with 10 ms ($= df^{-1}$) span each. One of the advantages of poloidal multi-point detection to single point measurement is that the poloidal flow direction can be determined. When the frequency is set to $f \geq 0$, the fluctuations with positive poloidal mode numbers flow in the electron diamagnetic direction and that with negative poloidal mode numbers flow in the ion diamagnetic direction.

The white asterisks in Fig. 3 show the calculated linear dispersion relation of drift waves with a uniform rotation by dc radial electric field assumed. The fluctuation peaks at (m, f) = (1, 2.8 kHz) and (2, 3.2 kHz) satisfy the dispersion relation, and they are considered to be drift wave modes. The peak at (m, f) = (–1, 0.9 kHz) is a flute wave-like mode in the ion diamagnetic direction. Other fluctuation peaks such as (m, f) = (2, 5.6 kHz) and (3, 4.7 kHz) do not satisfy the dispersion relation, and they are quasi-modes. The solid and broken lines in Fig. 3 show the frequency dependences of the mean poloidal mode number and its spread, respectively. They are defined by

$$\langle m(f)\rangle = \sum_m mS(m, f) \Big/ \sum_m S(m, f), \quad (1)$$

$$\Delta m(f)^2 = \frac{\sum_m [m - \langle m(f)\rangle]^2 S(m, f)}{\sum_m S(m, f)}. \quad (2)$$

The mean poloidal mode number traces the strong fluctuation peaks, and the spread decreases in the existence of the strong peaks. In the high frequency region with no remarkable fluctuation peaks ($f > 10$ kHz), the mean poloidal

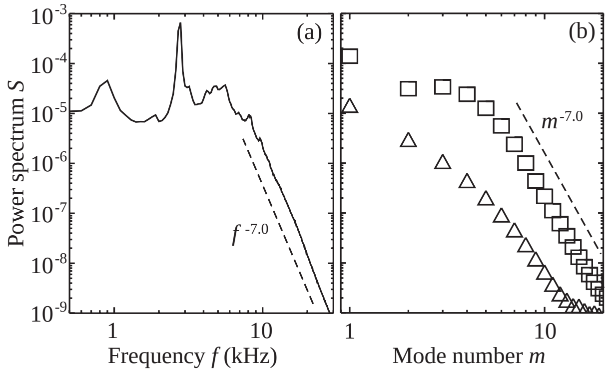

Fig. 4 One-dimensional power spectra (a) $S(f)$, (b) $S(m)$ (squares) and $S(-m)$ (triangles) (arb. unit). Dashed lines show the relationship $S \propto f^{-7.0}$ and $S \propto m^{-7.0}$.

mode number increases with the relationship $\langle m \rangle \propto f$ and the spread is an increasing function of f. These facts imply the existence of broadband components. The quasi-mode peaks and broadband components appear nearly on the line $\langle m \rangle \propto f$, and they are away from the linear dispersion relation curve of the drift wave. This is because nonlinear couplings between the parent modes force to excite quasi-mode peaks and broadband components in the position away from the dispersion relation. Thus, energy cascade to high m and high f region is expected [19].

Figure 4 shows the logarithmic plots of power spectra $S(f)$ and $S(m)$ calculated by integrating $S(m, f)$ with m and f, respectively. Both spectra have relations $S(f) \propto f^{-7.0}$ and $S(m) \propto m^{-7.0}$ in broadband regions ($f > 10$ kHz or $m > 5$). It is interesting that the decay laws are the same in the frequency and poloidal mode number spaces. It is also interesting that the power law of $S(m)$ is nearly equal to that led from the previous work (i.e., $S(m)^{0.5} \propto m^{-3.6}$ [3]). Although different experimental conditions induce individual eigen functions, the power laws in broadband regions become almost the same.

4 Broadband Fluctuation

Figure 5 shows the auto-correlation functions of the ion saturation current fluctuation in the frequency ranges of full-range and $f > 10$ kHz. Owing to the main fluctuation peaks, the auto-correlation time of the frequency of full-range is long (about the order of 10 ms). On the other hand, the auto-correlation time of the frequency of $f > 10$ kHz, which is in the broadband fluctuation region, is short (about the order of 1 ms). It means that the broadband fluctuation has a short time life than the main fluctuation peaks. Many short time fluctuations with various frequencies accumulate to form a broadband fluctuation.

Correlation length (poloidal angle) was calculated from the 64-channel data. Coherence coh of two time data

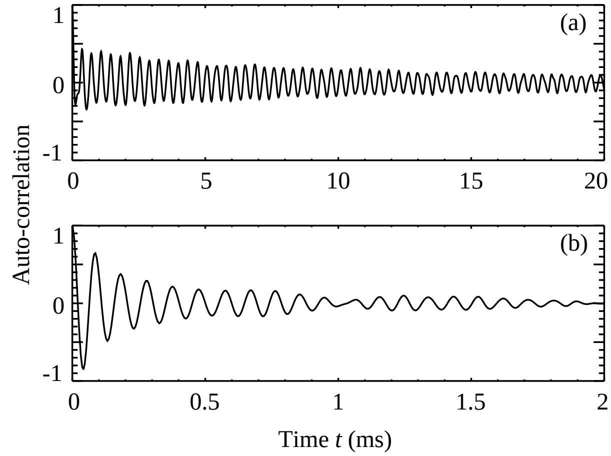

Fig. 5 Auto-correlation functions of the ion saturation current fluctuation in the frequency ranges of (a) full-range and (b) broadband region ($f > 10$ kHz).

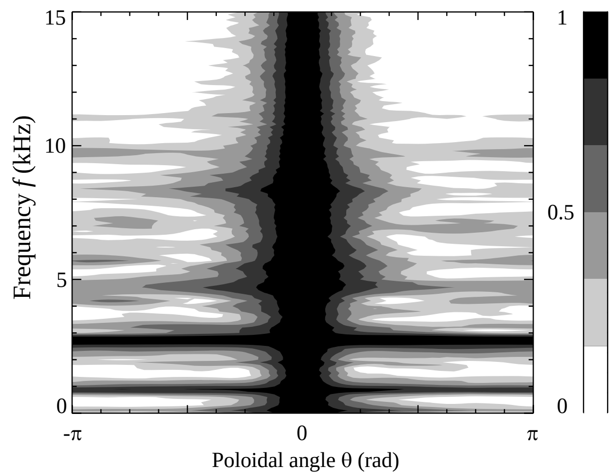

Fig. 6 Frequency dependence of the coherence in the poloidal angle space. Correlation length is long for fluctuation peaks and short for broadband fluctuation.

I_x and I_y is defined by

$$coh^2(f) = \frac{|S_{xy}(f)|^2}{S_{xx}(f)S_{yy}(f)}, \tag{3}$$

where $S_{xy} = \langle \hat{I}_x \hat{I}_y^* \rangle / df$. Correlation length is the distance where the coherences become e^{-1}. Figure 6 shows the frequency dependence of the coherence in the poloidal angle space. The coherence between different poloidal channels of the 64-channel probe array was calculated to produce Fig. 6. The correlation length in the poloidal direction is long for fluctuation peaks such as 0.9 kHz and 2.8 kHz, and is small (under $\pi/4$) for broadband fluctuation. The correlation length gradually decreases as the frequency becomes high. From this result, strong fluctuation peaks are produced globally in the poloidal direction, while broadband fluctuation is produced locally in the poloidal direction.

One of the features of our experiment is that two poloidal probe arrays are used for fluctuation measure-

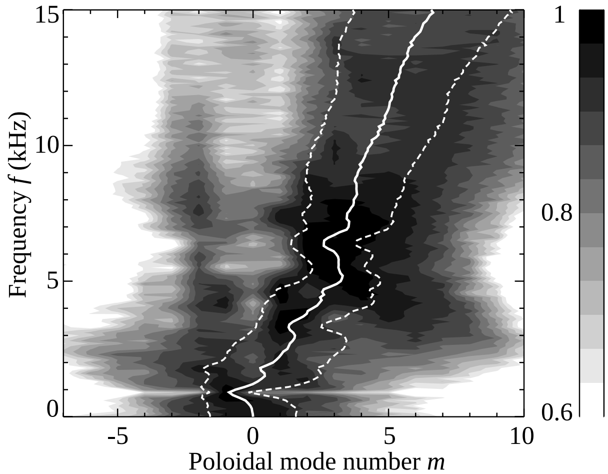

Fig. 7 Poloidal mode number decomposed axial coherence between the two poloidal probe arrays. The coherence is strong not only for fluctuation peaks but also for broadband fluctuation. The solid white line shows the mean poloidal mode number, and the broken white lines show its spread.

ments and so that quasi-two-dimensional measurement is available. By setting all of the measuring radii of the 48-channel probe array tips to 40 mm, poloidal analyses of the plasma column in separate of 0.26 m in the axial direction are performed. The 64-channel probe array can measure the poloidal mode number of $|m| \leq 32$, and the 48-channel probe array can measure $|m| \leq 24$. Although the two probe arrays have different numbers of probes, and many of the channels measure at different poloidal angles, the fluctuations of the poloidal mode number in the region $|m| \leq 24$ can be compared, and the poloidal mode number decomposed axial correlations can be calculated. Figure 7 shows the coherence between the two poloidal probe arrays in the poloidal mode number–frequency space. Compared with Fig. 3, it can be said that the coherence is strong not only for the fluctuation peaks such as drift wave modes, but also for broadband fluctuation even the spectral power is small. This fact suggests quasi-two-dimensional characteristics of the magnetized plasma turbulence

5 Summary

In summary, we have performed a measurement of drift wave turbulence in the LMD-U linear magnetized plasma by use of poloidal probe arrays. The obtained two-dimensional power spectrum $S(m, f)$ showed the excitation of drift wave modes and cascade to quasi-mode peaks and broadband components ($\langle m \rangle \propto f$ and $S \propto f^{-7.0}, m^{-7.0}$), which do not satisfy the linear dispersion relation of drift wave modes. The correlation time of the broadband fluctuation was shorter than that of the fluctuation peaks. The correlation length in the poloidal direction was short (under $\pi/4$) for broadband fluctuation, which suggests that this fluctuation is produced locally in the poloidal direction. Poloidal mode number decomposed axial coherence between the two poloidal probe arrays was calculated and showed that the broadband fluctuation and fluctuation peaks had strong axial coherences.

Acknowledgments

This work was supported by Grant-in-Aid for Specially-Promoted Research of MEXT (16002005) (Itoh Project), by Grant-in-Aid for Young Scientists (B) of JSPS (19760597), and by the collaboration programs of NIFS (NIFS07KOAP017) and of RIAM, Kyushu University.

[1] P.H. Diamond *et al.*, Plasma Phys. Control. Fusion **47**, R35 (2005).
[2] A. Yoshizawa, S.-I. Itoh and K. Itoh, *Plasma and Fluid Turbulence, Theory and Modelling* (Institute of Physics Publishing, Bristol and Philadelphia, 2003).
[3] A. Latten, T. Klinger and A. Piel, Rev. Sci. Instrum. **66**, 3254 (1995).
[4] T. Klinger *et al.*, Phys. Rev. Lett. **79**, 3913 (1997).
[5] M. Kono and M.Y. Tanaka, Phys. Rev. Lett. **84**, 4369 (2000).
[6] C. Schröder *et al.*, Phys. Rev. Lett. **86**, 5711 (2001).
[7] T. Kaneko, H. Tsunoyama and R. Hatakeyama, Phys. Rev. Lett. **90**, 125001 (2003).
[8] V. Sokolov and A.K. Sen, Phys. Rev. Lett. **92**, 165002 (2004).
[9] M.J. Burin *et al.*, Phys. Plasmas **12**, 052320 (2005).
[10] G.R. Tynan *et al.*, Plasma Phys. Control. Fusion **48**, S51 (2006).
[11] C. Lechte, S. Niedner and U. Stroth, New J. Phys. **4**, 34 (2002).
[12] Y. Nagashima *et al.*, Phys. Rev. Lett. **95**, 095002 (2005).
[13] Y. Hamada *et al.*, Phys. Rev. Lett. **96**, 115003 (2006).
[14] F.M. Poli *et al.*, Phys. Plasmas **13**, 102104 (2006).
[15] U. Stroth *et al.*, Phys. Plasmas **11**, 2558 (2004).
[16] S. Shinohara *et al.*, *Proc. 28th Int. Conf. on Phenomena in Ionized Gases* (Institute of Plasma Physics AS CR, Prague, 2007), 1P04-08.
[17] K. Terasaka *et al.*, Plasma Fusion Res. **2**, 031 (2007).
[18] N. Kasuya *et al.*, J. Phys. Soc. Jpn. **76**, 044501 (2007).
[19] T. Yamada *et al.*, submitted to Plasma Fusion Res.
[20] T. Yamada *et al.*, submitted to Rev. Sci. Instrum.